LA-UR-09-04023

Title: The CTOF Measurements and Monte Carlo Analyses of Neutron Spectra for Backward Direction from Iron Target Irradiated by Protons with Energies from 400 to 1200 MeV

Author(s): I. L. Azhgirey, V. I. Belyakov-Bodin, I. I. Degtyarev, S. G. Mashnik, F. X. Gallmeier, and W. Lu

Intended for: Nucl. Instrum. Meth. B 267 (2009) 3601;
E-print: arXiv:0907.0181

Los Alamos
NATIONAL LABORATORY
EST.1943

Nuclear Instruments and Methods in Physics Research B 267 (2009) 3601–3605

Contents lists available at ScienceDirect

Nuclear Instruments and Methods in Physics Research B

journal homepage: www.elsevier.com/locate/nimb

CTOF measurements and Monte Carlo analyses of neutron spectra for the backward direction from an iron target irradiated with 400–1200 MeV protons

I.L. Azhgirey [a], V.I. Belyakov-Bodin [a,*], I.I. Degtyarev [a], S.G. Mashnik [b], F.X. Gallmeier [c], W. Lu [c]

[a] Institute for High Energy Physics, Protvino, Russian Federation
[b] Los Alamos National Laboratory, Los Alamos, NM 87545, USA
[c] Oak Ridge National Laboratory, Oak Ridge, TN 37830, USA

ARTICLE INFO

Article history:
Received 27 May 2009
Received in revised form 16 September 2009
Available online 23 September 2009

PACS:
29.30.Hs
29.85.Fj

Keywords:
Measurement
Neutron spectrum
Comparison
Prediction by the MARS and the MCNPX code systems

ABSTRACT

A calorimetric-time-of-flight (CTOF) technique was used for real-time, high-precision measurement of the neutron spectrum at an angle of 175° from the initial proton beam direction, which hits a face plane of a cylindrical iron target of 20 cm in diameter and 25 cm thick. A comparison was performed between the neutron spectra predicted by the MARS and the MCNPX codes and that measured for 400, 600, 800, 1000 and 1200 MeV protons.

1. Introduction

The MARS and the MCNPX codes are useful tools for the analysis and design of systems incorporating high-intensity neutron sources such as an accelerator-driven system (ADS). These codes simulate the transport of particles in matter with cascading secondary particles over a wide energy range. This encompasses the ability to determine the neutron spectrum around a system. For many system designs, and especially for high-energy, high beam current applications, an important design factor is the neutron spectrum emitted from the ADS target. Consequently, it is important that the accuracy for neutron spectrum predictions by the codes is well determined. The goal of this study is to determine the precision of the MARS and the MCNPX codes in making these predictions at a wide angle.

The geometry for both codes which modeled the experimental configuration consists of a cylindrical target and a detecting volume. The aim of our work was to investigate neutron spectra only in backward direction; therefore we chose 175° as a suitable angle. There are several reasons why we limited ourselves to only the backward angle of 175°. First, we need such information for programmatic needs, for shielding considerations, to be able to prevent cases when personnel may receive radiation from backward fluxes, as once happened at BNL. Second, it is much more difficult for all models to describe particle production at very backward angles than at intermediate or forward angles. Our data allow us to test event-generators used by transport codes in this "difficult" kinematics region. Third, spectra of secondary particles at very backward angles are of great academic interest, to understand the mechanism of cumulative particle production, under investigation for almost four decades, but still with many open questions.

2. Facility description and operation principle

A detailed description of the experimental facility construction, the calorimetric-time-of-flight (CTOF) technique, method of data taking, and experimental results for tungsten target irradiated by protons was recently given [1,2]. Therefore, only a brief description of the ZOMBE facility and the CTOF technique are needed for understanding the problem is presented in this paper.

We used a proton beam extracted from the U-1.5 ring accelerator (booster) in the Institute of High Energy Physics, Protvino, by a tripping magnet. The booster cycle time was about 9 s containing

* Corresponding author. Tel.: +8 962 944 3801.
E-mail address: vl.i.belyakov-b@mail.ru (V.I. Belyakov-Bodin).

0168-583X/$ - see front matter © 2009 Elsevier B.V. All rights reserved.
doi:10.1016/j.nimb.2009.09.019

29 pulses of about 30 ns long, each containing 1.3×10^{11} protons. The extraction time is 1.6 s. Beam intensity measurements were carried out for each pulse using an induction current sensor [3] with an accuracy of about 7%. The proton beam energy values were determined with an error of ~0.5% in the proton energy value. The average radial distribution of protons in the beam has been obtained for this experiment [1,2] and was compatible with a Gaussian of a full-width at half-maximum of 24 mm. A proton beam hits a face plane of target placed on the ZOMBE facility (see Fig. 1). The target axis position was superimposed on the geodesic beam axis.

The CTOF technique consists of a set of current mode time-of-flight instruments each having a set of organic scintillation detectors placed at a different distance from a source at an angle of interest away from the beam direction. One litre ($10 \times 10 \times 10\ cm^3$) organic scintillators were used as the detectors. The first detector was placed at distance 8.7 m from the face plane of the target at 175° to the proton beam direction. The second detector was placed at distance of 29 m at the same angle. There are only two directions into the booster-room (175° and 96°) where long-distance (more then 26 m) detectors may by placed for measurements of high-energy neutrons. Wavelength shifters were coupled with the scintillators and its output signals were transported to each photo-multiplier tube (PMT) by a 120 m long light-guide (LG). The PMT outputs were digitized by a TDS 3034b oscilloscope (0.4 ns resolution, 200 MHz bandwidth). The data were obtained within a time of 2000 ns from the start of the irradiation cycle and sent to an off-line computer for further analyses. Since the oscilloscope resolution is 0.4 ns, there are so many experimental points that the neutron spectra in Figs. 4–8 appear as continuous lines.

All of the beam pickup signals were digitized for reconstruction of the average proton beam intensity as a function of time. In the measurements, 5000 proton beam pulses were used to average the photometric signals. To exclude any radiation-induced noise from the photometric signals of the detectors, such as neutrons reflected from the walls, ceiling and floor, radiation from the accelerator, and so on, it was necessary to make additional measurement for the case when the burst source overshadowed the detector cylindrical shield. For the shield we used a set of 45 cm thick iron and 40 cm thick tungsten discs, both 20 cm in diameter. We have the option of using only one shield in some experiments, so we used one for the 175°-direction in this experiment.

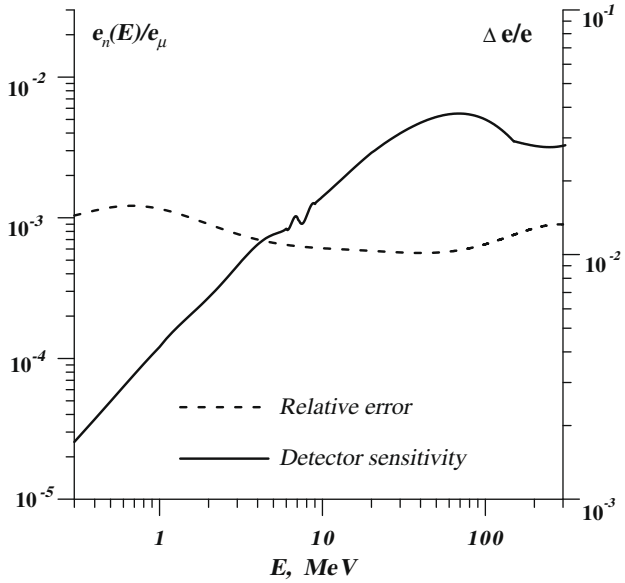

Fig. 2. Detector sensitivity to neutron; solid line corresponds to the left scale while dashed line, to the right one.

The difference of these two measurements will give a pure signal from the source. The amplitude of a light signal in a detector caused by a nonzero-mass particle is:

$$u(t) = k \cdot S(E) \cdot e_f(E) \cdot dE/dt,$$

where $S(E)$ is the energy spectrum of particles emitted from a target, $e_f(E)$ is the sensitivity of the detector, dE/dt is the time derivative of the particle energy for r-distance detector, and k is a coefficient. The sensitivity of the detector to neutrons (and cosmic μ-mesons ($e\mu$) was calculated by the RTS&T code [4], see Fig. 2. We used the time integral of a photometric signal of the scintillator caused by a cosmic μ-meson signal for determination of the k-coefficient, i.e. for absolute calibration of the detectors.

The digitized voltage amplitude is determined by the following integral equation:

$$U(t) = u(t)^* \cdot p(t)^* \cdot d(t)^* \cdot LG(t)^* \cdot PMT(t), \quad (1)$$

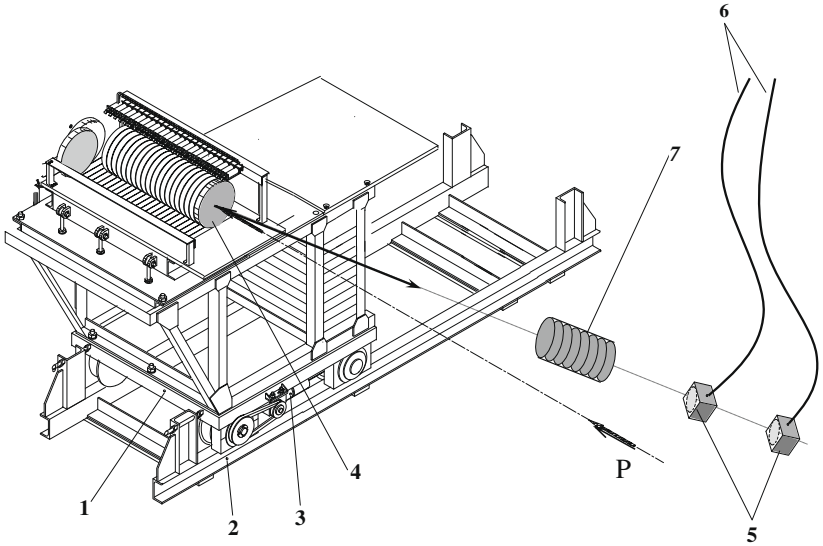

Fig. 1. Scheme of the ZOMBE facility: (1) mobile test bench; (2) rails; (3) bench displacement motor; (4) target; (5) detectors; (6) light-guide; (7) local shield; and P – proton beam direction.

where $p(t)$ is the proton beam intensity as a function of time; $d(t)$, $LG(t)$, and $PMT(t)$ are pulse functions of the detector, LG, and PMT, respectively; and the asterisk $(^*)$ is a convolution transform symbol:

$$u(t)^* \cdot p(t) = \int_o^t u(\xi) \cdot p(t-\xi) d\xi.$$

An original code was made for determining the $u(t)$ function from Eq. (1) by using $U(t)$, $p(t)$, $d(t)$, $LG(t)$, and $PMT(t)$.

The part of the photometric signal caused by gamma rays from the target was extracted in the following manner. The time structure of this part of the signal does not depend on the distance between the source and detector. Therefore, we determined this shape from the distant detector signal, which could be separated easily and clearly into gamma rays and nucleon components for the detector with a lead filter. The part of the photometric signal caused by the proton flux can be extracted from the total photometric signal by inserting different kinds of filters between the detector and the spallation source. We used two detectors at distance of 29 m, each with and without a lead filter. The photometric signal from the detector without a filter was subtracted from the gamma- and proton-induced signals to obtain the neutron component up to 13 MeV. It is possible to reduce the relative error for the low-energy part of these signals and expand the energy range, for example, by improving the light system and by using a better digitizing oscilloscope. Nevertheless, measurements were conducted also by using a detector at 8.7 m to give the neutron spectrum below 13 MeV, because it was easier. The total relative error including beam intensity, beam energy, detector sensitivity, and photometric signal errors for 0.4- and 1.2-GeV protons are presented on Fig. 3.

3. Monte Carlo simulation

The MCNPX calculated backscattering neutron spectra in Figs. 4–8 were performed with version 2.6.0 [5] using the Bertini INC

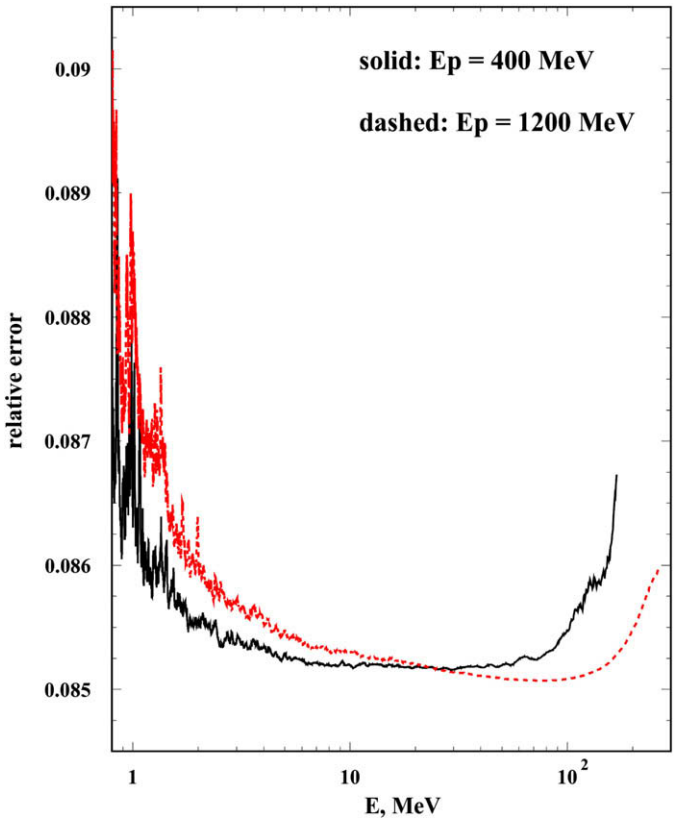

Fig. 3. Relative errors for experimental neutron spectrum.

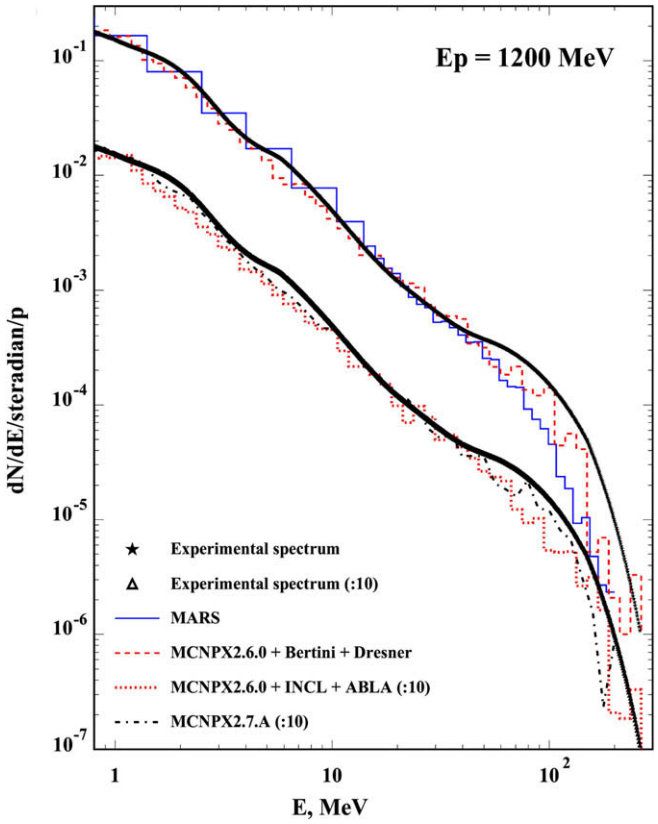

Fig. 4. Experimental neutron spectrum for 1.2 GeV initial proton energy and calculation by the MARS code and the MCNPX code.

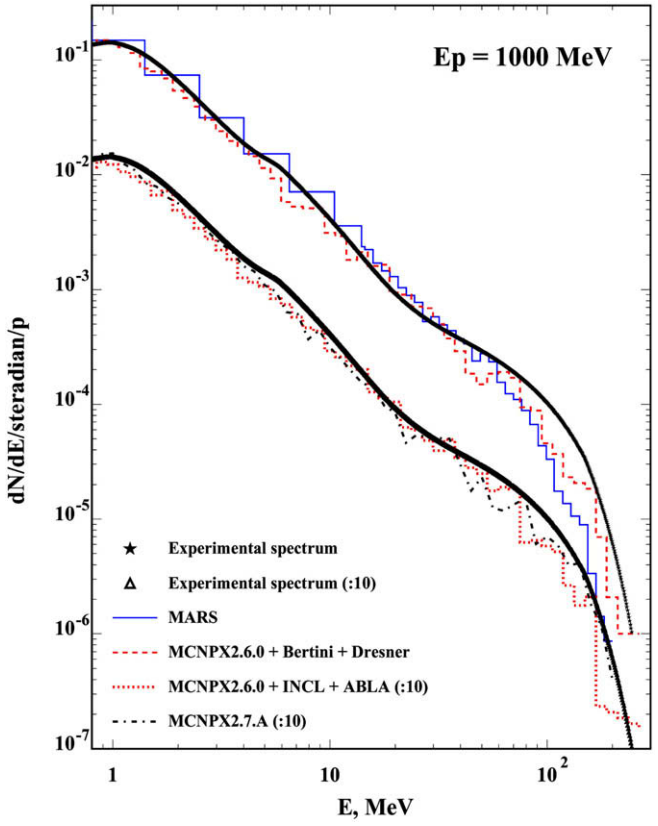

Fig. 5. Experimental neutron spectrum for 1.0 GeV initial proton energy and calculation by the MARS code and the MCNPX code.

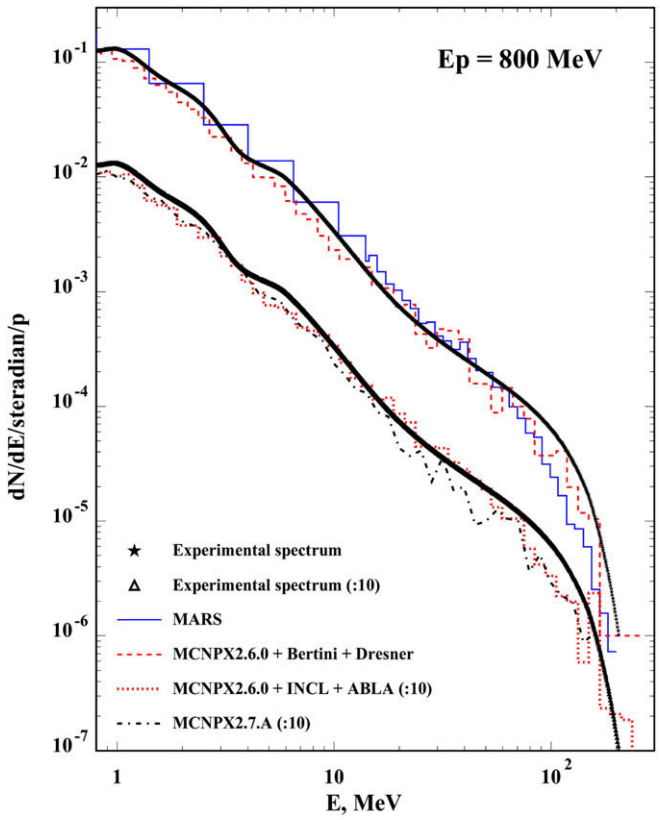

Fig. 6. Experimental neutron spectrum for 0.8 GeV initial proton energy and calculation by the MARS code and the MCNPX code.

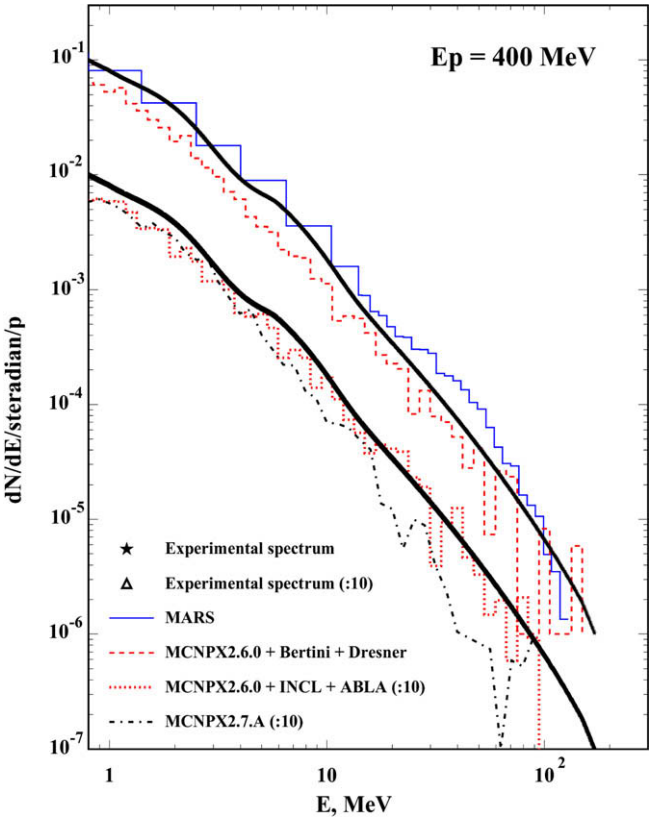

Fig. 8. Experimental neutron spectrum for 0.4 GeV initial proton and calculation by the MARS code and the MCNPX code.

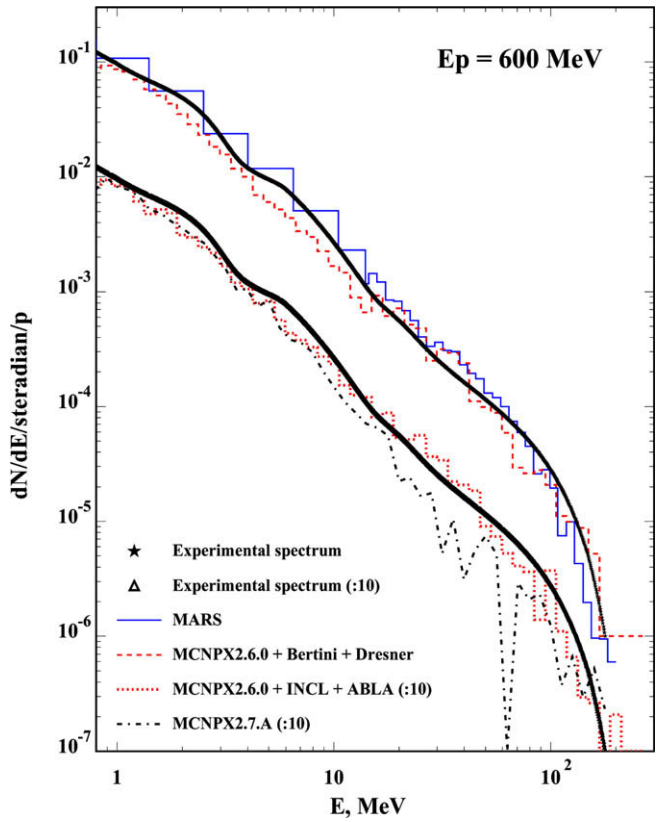

Fig. 7. Experimental neutron spectrum for 0.6 GeV initial proton energy and calculation by the MARS code and the MCNPX code.

[6] coupled with the Dresner evaporation model [7] (MCNPX defaults, using also the multistage pre-equilibrium model, MPM [8]), the Liege INC model INCL4 [9] merged with the GSI evaporation/fission model ABLA [10], as well as the 03.01 version of the Cascade-Exciton Model event-generator CEM03.01 [11,12] using an improvement of the Generalized Evaporation Model GEM2 by Furihata [13] to calculate evaporation/fission and its own Modified Exciton Model (MEM). A newer version, MCNPX 2.7.A [14] with the latest implementation CEM03.02 [12,15] was also used. We note that all neutron spectra calculated with MCNPX 2.6.0 using CEM03.01 are very similar to those obtained with MCNPX 2.7.A using CEM03.02, so we present below only results using CEM03.02. For the proton and neutron transport and interactions up to 150 MeV, MCNPX in all cases uses applied tabulated continuous-energy cross sections from the LA150 proton and neutron libraries. The calculation assumed a Gaussian-distributed incident proton beam with a FWHM of 2.4 cm hitting a cylindrical iron target. The radius of the iron target is 10 cm and the length is 25 cm. The backscattered neutrons were tallied at an angle of 175° of the incident beam direction and at 6 m upstream of the front surface of the target. A ring surface tally was adopted to improve the efficiency of the simulation by taking advantage of the symmetry.

The MARS code [16] simulates a process of development of the nuclear-electromagnetic cascades in matter. Its physical module is based mostly on parameterization of the physical processes. It provides flexibility and rather high operation speed for engineering applications and optimization tasks. MARS is used for radiation-related modeling at accelerators, such as shielding design [17], dose distribution and energy deposition simulations [18], and radiation background calculations [19]. In this region of the primary proton energy (below 5 GeV), MARS uses a phenomenological model for the production of secondary particles in inelastic hadron-nucleus

interactions [20]. For low-energy neutron transport at energies below a 14.5 MeV threshold and down to the thermal energy, MARS uses a multi-group approximation and a 28 group library of neutron constants.

In the MARS cascade model, charged particles (protons and pions) are absorbed locally when their kinetic energy falls below 10 MeV. At an energy of 10 MeV, proton and pion ionization ranges in iron are more than two orders of magnitude less than the average path before inelastic interaction with the nuclei. Therefore for our initial beam energies from 400 to 1200 MeV we neglect secondary interactions caused by sub-threshold charged hadrons, because it can contribute only small additions to the neutron spectrum, formed mainly by the interactions of high-energy particles.

The target was considered as a solid iron cylinder with a length of 25 cm and diameter of 20 cm. A detecting volume of $10 \times 10 \times 10$ cm^3 was placed 9 m upstream of the target front face plane, and the angle between beam direction and direction from target to detector is 175°. A Gaussian distribution of the proton beam with $\sigma_{x,y} = 1.4$ cm was used, which is an approximation of the measured distribution. Test runs show no difference in spectra between a point-like beam and a realistic distribution. The space between the target and detector was filled with air.

4. Comparison of experimental and calculation results

As shown in Figs. 4–8, MARS results agree well with the measured spectra and the MCNPX results. MARS overestimates a little the 20–80 MeV portion of the spectra at 400 MeV and underestimates the high-energy tails of the spectra at 800, 1000, and especially at 1200 MeV. All event-generators of MCNPX underestimate a little the measured spectra in the ~5–10 MeV energy region, as well as at high energies, at the very end of the spectra tails, and also a little, at very low energies, in the 1–3 MeV region. The overall agreement of results by different event-generators with the measured spectra depends mostly on the proton incident energy: CEM tends to agree better with the data at high energies of 1 and 1.2 GeV, while Bertini & Dresner and INCL and ABLA, as a rule, agree better with the data at lower incident energies.

A small difference is observed for neutron energies from several MeV to ~50 MeV, where a shoulder is present on the measured spectra around 5 MeV showing higher backscattered neuron flux compared to the MCNPX calculated spectra for neutrons from several MeV to 10 MeV and lower neutron flux for neutrons above 10 MeV up to ~50 MeV. Neither event-generators (CEM03 and BERTINI & Dresner) using their own, different pre-equilibrium models, nor the INCL & ABLA, which does not use a pre-equilibrium stage, are able to capture this shoulder. Such a shoulder on the measured spectrum probably indicates the superposition of the flux from the low-energy evaporation neutrons and high-energy cascade neutrons. Although the high-energy cascade neutron flux calculated by all models of MCNPX agrees reasonably well with the measurement at incident proton energies above 400 MeV, all the MCNPX event-generators used here underestimate slightly the measured spectrum at 400 MeV, up to a factor of two.

MARS underestimates the high-energy tails of spectra at the highest beam energies. It produces ~3× less neutrons compared to the data. Such behavior for this kinematical region is similar to that for a tungsten target [2].

We now comment on a still open question. Our data indicate a small shoulder around 4–10 MeV which is seen in practically all measured neutron spectra. A similar situation was observed also for a tungsten target [2], and none of the models we tested so far reproduced well this feature. We do not have yet a good understanding of this situation, as several combined effects could contribute to this feature for thick targets. Further investigations, including using other nuclear reaction models and probably more measurements are needed to solve this problem. We cannot solve it by comparing our results with previous measurements and calculations simply because we do not know of any previous studies of neutron spectra from thick targets at 175°. To the best of our knowledge, only the SATURNE measurements by David et al. [21] on thick iron targets at 0.8, 1.2, and 1.6 GeV analyzed with the INCL4 & ABLA and Bertini & Dresner event-generators are similar to our work. The largest angle measured at SATURNE was only 160°, and the target dimensions were different, so we cannot compare directly our results with Ref. [21]. While a similar measurement of neutron spectra from thick targets bombarded by proton energies similar to ours was done by Miego et al. at KEK [22], but the targets were of lead and the proton energies were 0.5 and 1.5 GeV, so we cannot compare our results with theirs.

Acknowledgements

We are grateful to G.A. Losev and A.V. Feofilov (both of the Institute for High Energy Physics) for providing the beam so reliably under the conditions demanded for this experiment. This work was partially supported by the US DOE.

References

[1] V.I. Belyakov-Bodin et al., Nucl. Instrum. Methods A 465 (2001) 346.
[2] V.I. Belyakov-Bodin et al., Nucl. Instrum. Methods A 596 (2008) 434.
[3] I.M. Bolotin et al., Radio Technical Institute of Academy of Science report RTI AS USSR-35, 1980 (in Russian).
[4] A.I. Blokhin et al., RTS&T Monte Carlo code (facilities and computation methods), in: Proceedings of the SARE-3 Workshop, KEK, Tsukuba, Japan, 1997.
[5] J.S. Hendricks et al., MCNPX 2.6.0 Extensions, LANL Report LA-UR-08-2216, Los Alamos, 2008. <http://mcnpx.lanl.gov/>.
[6] H.W. Bertini, Phys. Rev. 131 (1963) 1801;
H.W. Bertini, Phys. Rev. 188 (1969) 1711.
[7] L. Dresner, ORNL-TM-196, 1962;
P. Cloth et al., Kernforschungsanlage Jülich Report Jül-Spez-196, 1983.
[8] R.E. Prael, M. Bozoian, LANL Report LA-UR-88-3238, Los Alamos, 1988.
[9] A. Boudard et al., Phys. Rev. C 66 (2002) 044615.
[10] A.R. Junghans et al., Nucl. Phys. A 629 (1998) 635.
[11] S.G. Mashnik et al., LANL Report LA-UR-05-7321, Los Alamos, 2005, RSICC Code Package PSR-532. <http://www-rsicc.ornl.gov/codes/psr/psr5/psr532.htm>.
[12] S.G. Mashnik et al., LANL Report LA-UR-08-2931, Los Alamos, 200, Eprint: arXiv:0805.0751.
[13] S. Furihata, Nucl. Instrum. Methods B 171 (2000) 252.
[14] D.B. Pelowitz et al., MCNPX 2.7.A Extensions, LANL Report LA-UR-08-07182, Los Alamos, 2008. <http://mcnpx.lanl.gov/>.
[15] S.G. Mashnik et al., Research Note X-3-RN(U)-07-03, LANL Report LA-UR-06-8652, Los Alamos, 2007. <http://mcnpx.lanl.gov/>.
[16] I. Azhgirey, V. Talanov, The status of MARS program complex, in: Proceedings of the XVIII Workshop on the Charged Particles Accelerators, vol. 2, Protvino, 2000, pp. 184–187.
[17] I. Azhgirey, V. Talanov, Analyzing the efficiency of the forward radiation shielding for the CMS detector at the LHC, Instrum. Exp. Technol. 45 (4) (2002) 509–515.
[18] V.I. Belyakov-Bodin, I.L. Azhgirey, I.I. Degtyarev, Instrum. Methods A 572 (2007) 935.
[19] R. Appleby et al., Machine induced backgrounds for FP420, in: Proceedings of EPAC08, Genoa, Italy, May 2008, pp. 559–561.
[20] B.S. Sychov, A.Ya. Serov, B.V. Man'ko, Preprint MRTI No. 799, Moscow, 1979.
[21] J.-C. David et al., Spallation neutron production on thick target at saturne, in: A. Kelic, K.-H. Schmidt (Eds.), Proceedings of the Workshop on Nuclear Data for the Transmutation of Nuclear Waste, GSI-Darmstadt, Germany, 1–5 September, 2003, ISBN:3-00-012276-1. <http://www-wnt.gsi.de/tramu/>.
[22] S. Meigo et al., Nucl. Instrum. Methods A 431 (1999) 521.